

Numerical Simulation of Zonal Disintegration for Deep Rock Mass under High Geostress

Qiang Gao^{1,*}, Qiangyong Zhang¹, Wen Xiang¹ and Xutao Zhang²

¹Geotechnical and Structural Engineering Research Centre, Shandong University, Jinan, China

²School of Architecture and Engineering, Liaocheng University, Liaocheng, China

*Corresponding author e-mail: gaoqiangsdu@163.com

Abstract. As a common phenomenon of deep underground engineering under high geostress, the generation and evolution of zonal disintegration phenomenon (ZDP) are analyzed by means of numerical simulation. Based on the strain gradient theory and the deformation theory of plasticity, an elastoplastic damage softening model is put forward. In terms of maximum tensile stress criterion and strain energy density failure theory, the element failure criteria have been developed to simulate the failure behavior of rock mass. The zonal disintegration code has been developed by the FORTRAN of ABAQUS. Then it was used to determine the failure pattern of the rock mass around the deep cavern and the quantity and width of the fractured zones also have been obtained. The numerical calculation results are in good agreement with the model test measurements.

1. Introduction

With the rapid economic development and increasing energy demand, many engineering constructions such as mining engineering, traffic engineering and large-scale hydropower engineering are entered into high geostress and complex deep geological environments. The mechanical properties and the deformation failure mode of deep rock masses are different from the shallow rock mass in which the zonal disintegration phenomenon (ZDP) is an important feature of the deep rock mass [1].

The ZDP has been confirmed by physical detection methods in the excavation of deep caverns. The resistivity meters were used in the deep mine of Taimyrskii to detect the zonal disintegration [2]. Borehole televisions were adopted to monitor the ZDP in the Huainan coal mine [3]. Many model tests are implemented to study this phenomenon. The ZDP is going to happen under the effect of large axial pressure and the undulations of internal rock strain and displacement law are measured [4, 5]. Meanwhile, a series of numerical simulation analysis are conducted to expound the gradual formation of ZDP in the surrounding rock of the cavern [6, 7].

With the deepening of theoretical research, the zonal disintegration is a special strain localization phenomenon with obvious regularity and the theory of strain gradient is more reasonable and accurate to study the mechanism of the zonal disintegration mechanism of surrounding rock under high geostress. The coupled stress theory was applied to the study of jointed rock masses [8], and the effect of strain gradient on post-peak deformation of rock mass was considered to analyze the mechanical characteristics of zonal disintegration [9].



In summary, the ZDP of deep rock masses has been confirmed in engineering sites and indoor model tests, and many theories have been proposed to explain this kind of damage phenomenon. But so far, most theories do not consider the role of strain gradient on deep caverns. Based on the strain gradient theory and the damage softening model, an elastoplastic softening model is established. In terms of maximum tensile stress criterion and strain energy density theory, the element failure criteria have been developed to simulate the failure behavior of rock. The zonal disintegration code has been developed by the UMAT of ABAQUS. Then it was used to determine the failure pattern of the rock mass around the deep cavern and the results of numerical simulation can well simulate the zonal disintegration that occurs in the deep rock mass.

2. Elastoplastic damage softening model with strain gradient

2.1. Nonlinear Softening Constitutive Relation of Uniaxial Compression

With the development and utilization of underground space, the excavation depth is extended, and the failure of deep rock mass presents the characteristics of ductility and strain softening under the condition of high geostress [10]. The stress-strain curve of uniaxial compression is shown in Fig. 1.

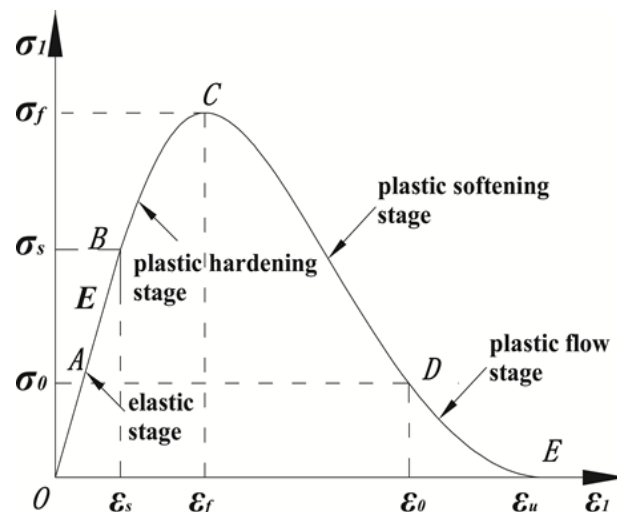


Figure 1. Stress-strain curve of uniaxial compression

The OA stage is called as the stage of cracks compaction, and the cracks inside the rock mass are continuously compacted and closed under the action of external force. The AB stage is linear elastic, and the point B is the yield point which represents the dividing line or transition from the elastic to the plastic region of the curve. σ_s is yield stress and ε_s is yield strain. The original cracks are pressed and the new cracks are produced. In general, the stress-strain curve needs to be properly simplified in theoretical analysis. OA and AB are collectively simplified linear elastic region, and the slope is the elastic modulus E .

The BC stage is a stage of plastic hardening. The point C is the point of peak strength, σ_f is the peak stress, and ε_f is the peak strain. In general, the stage is short. The stress-strain curves show obvious nonlinearity with the convergence and penetration of the crack accelerating expansion. The CD stage is the stage of plastic softening, and the point of D is the intersection of the softening stage and the fluid stage, which σ_0 is the residual stress and ε_0 is the residual strain. At this stage, numerous cracks are generated, which tend to coalesce into macro - main cracks. The BC and CD can be collectively regarded as plastic bearing region [11].

The DE stage is the residual stage, the strength of the rock mass declines with the increase of deformation. Until the deformation reaches the ultimate strain ε_u , the rock mass is completely destroyed.

In the elastic stage, the constitutive equation can be expressed as the following form:

$$\sigma_1(\varepsilon_1) = E\varepsilon_1 \quad (\varepsilon_1 < \varepsilon_s) \quad (1)$$

Where, σ_1 is the first principal stress, ε_1 is the first principal strain. E is the elastic modulus.

In the plastic stage, the constitutive equation of undamaged rock mass is in the following exponential form [12, 13]:

$$\sigma_1(\varepsilon_1) = (1 - \delta D)E_0 \left[\varepsilon_1 \exp(k_1 \varepsilon_1) + k_2 / \varepsilon_1 \right] \quad (\varepsilon_1 \geq \varepsilon_s) \quad (2)$$

where, k_1 and k_2 are the small parameter perturbation terms, which is a smooth connection between the plastic hardening stage and the elastic stage, E_0 is the undetermined parameters, D is the damage variable and the evolution function can be described with the following damage evolution law [14]:

$$D = D(\varepsilon_1) = \begin{cases} 0, & \varepsilon_1 < \varepsilon_s \\ \frac{\varepsilon_u}{\varepsilon_1} \frac{\varepsilon_1 - \varepsilon_s}{\varepsilon_u - \varepsilon_s}, & \varepsilon_s \leq \varepsilon_1 < \varepsilon_u \\ 1, & \varepsilon_1 \geq \varepsilon_u \end{cases} \quad (3)$$

2.2. Deformation Theory of Plasticity

In plastic mechanics, the representation of the Hencky deformation theory [15] can be written as:

$$\tilde{\sigma} = 3H \tilde{\varepsilon} \quad (4)$$

Where, $\tilde{\sigma}$ and $\tilde{\varepsilon}$ are the equivalent stress and strain. In particular, the expressions $\tilde{\sigma} = \sigma_1$ and $\tilde{\varepsilon} = \varepsilon_1$ are established under uniaxial compression [16]. $H = H(\tilde{\varepsilon})$ is a function relation that represents about $\tilde{\varepsilon}$, which is irrelevant to simple or complex stress state.

After substituting Eq. (4) into Eq. (2), the following function relation can be given:

$$H = \tilde{\sigma} / (3\tilde{\varepsilon}) = (1 - \delta D) / 3 \cdot E_0 \left[\exp(k_1 \tilde{\varepsilon}) + k_2 / \tilde{\varepsilon}^2 \right] \quad (5)$$

According to Eq. (5), the constitutive equation can be represented as the following form:

$$\tilde{\sigma} = (1 - \delta D)E_0 \left[\tilde{\varepsilon} \exp(k_1 \tilde{\varepsilon}) + \frac{k_2}{\tilde{\varepsilon}} \right] \quad (\tilde{\varepsilon} \geq \varepsilon_s) \quad (6)$$

In order to unify the constitutive equation in form, the relation between equivalent stress and strain in elastic area is obtained as follows:

$$\tilde{\sigma} = 3G \tilde{\varepsilon} \quad (\tilde{\varepsilon} < \varepsilon_s) \quad (7)$$

Where, $G = E / (2(1 + \nu))$, G is Lamé constants, E is elastic modulus, ν is Poisson ratio.

Therefore, the elastoplastic damage softening constitutive model of rock mass is established as follows:

$$\tilde{\sigma} = \begin{cases} 3G\tilde{\varepsilon} & (\tilde{\varepsilon} < \varepsilon_s) \\ (1 - \delta D)E_0 \left[\tilde{\varepsilon} \exp(k_1 \tilde{\varepsilon}) + \frac{k_2}{\tilde{\varepsilon}} \right] & (\tilde{\varepsilon} < \varepsilon_s) \end{cases} \quad (8)$$

2.3. Strain Gradient and the Generalized Equivalent Stress and Strain

The ZDP in deep rock is a kind strain localization phenomenon with obvious regularity, and the strain gradient theory maintains advantage in the study of the localization of the strain, so the analysis of ZDP should consider the influence of strain gradient.

In the Toupin-Mindlin strain gradient theory [17, 18], the total strain consists of two parts: the conventional Eulerian strain tensor ε_{ij} and the high order strain tensor η_{ijk} . The specific formulae of ε_{ij} and η_{ijk} are deduced as:

$$\varepsilon_{ij} = (u_{i,j} + u_{j,i}) / 2, \quad \eta_{ijk} = \partial_i \partial_j u_k = u_{k,ij} \quad (9)$$

Where, u_i is the macroscopic displacement of material.

The constitutive equation of Toupin-Mindlin strain gradient theory can be written as:

$$\begin{cases} \sigma_{ij} = \lambda \varepsilon_{kk} \delta_{ij} + 2G \varepsilon_{ij} \\ \tau_{ijk} = \frac{1}{4} G l^2 \left[(7\eta_{ijk} + \eta_{kji} + \eta_{kij}) + (2\eta_{kpp} + 4\eta_{ppk}) \delta_{ij} \right. \\ \left. + (2\eta_{ipp} + \eta_{ppi}) \delta_{jk} + (2\eta_{jpp} + \eta_{ppj}) \delta_{ik} \right] \end{cases} \quad (10)$$

Where, σ_{ij} is two order Cauchy stress tensor, which is conjugate to the Eulerian strain tensor ε_{ij} , τ_{ijk} is set as the three order stress tensor which is conjugate to strain gradient tensor η_{ijk} . δ_{ij} is the Kronecker symbol, λ and G are the lamé constant, l is the internal length parameter, which is generally valued as diameter of aggregate particles [19].

The expressions of the generalized equivalent stress and strain containing the strain gradient [20] are represented as:

$$\tilde{\varepsilon} = \sqrt{\frac{2}{3} e_{ij} e_{ij} + l^2 \eta_{ijk} \eta_{ijk}}, \quad \tilde{\sigma} = \sqrt{\frac{3}{2} S_{ij} S_{ij} + l^{-2} \tau_{ijk} \tau_{ijk}} \quad (11)$$

Where, $e_{ij} = \varepsilon_{ij} - \varepsilon_m \delta_{ij}$, $\varepsilon_m = (\varepsilon_{11} + \varepsilon_{22} + \varepsilon_{33}) / 3$, $S_{ij} = \sigma_{ij} - \sigma_m \delta_{ij}$, $\sigma_m = (\sigma_{11} + \sigma_{22} + \sigma_{33}) / 3$.

3. Failure Criterion of ZDP

3.1. Tensile failure

When the maximum tensile stress σ_i of the surrounding rock reaches the tensile strength σ_t , the base elements of rock mass occur tensile failure. The elastic modulus is reduced to a small residual value E_c^* , which is $E_c^* = 0.05E$.

3.2. Strain energy density failure theory

According to the strain energy density theory [21] and the effect of strain gradient, the strain energy density of each element can be expressed by the following equation under isothermal conditions.

$$dW/dV = \int_0^{\varepsilon_{ij}} \sigma_{ij} d\varepsilon_{ij} = \frac{1}{2} \lambda \varepsilon_{ii} \varepsilon_{jj} + G \varepsilon_{ij} \varepsilon_{ij} + \frac{1}{8} G l^2 (4\eta_{ijj} \eta_{ikk} + 4\eta_{iik} \eta_{kjj} + 4\eta_{iik} \eta_{jjk} + 7\eta_{ijk} \eta_{ijk} + 2\eta_{ijk} \eta_{kji}) \quad (12)$$

The above equation shows that the strain energy density is determined by the deformation history of stress σ_{ij} , strain increment ε_{ij} and strain gradient tensor η_{ijk} .

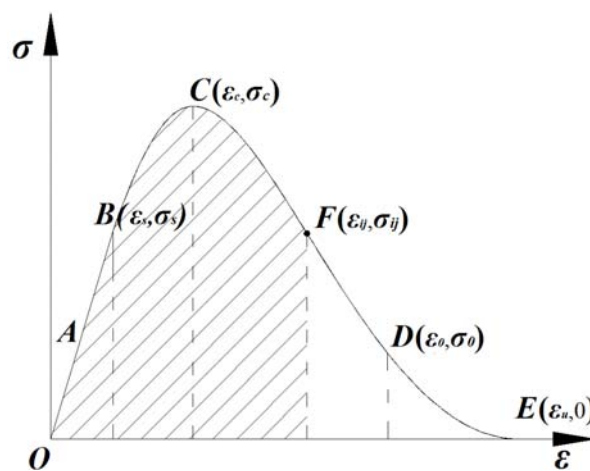


Figure 2. The curve of strain energy density

As shown in Fig. 2, the damage and failure criterion of rock based on strain energy density is expressed as follows:

(1) When $(dW/dV) < (dW/dV)_B = \int_0^{\varepsilon_s} \sigma_{ij} d\varepsilon_{ij}$ (ε_s is the yield strain in the stress process), $(dW/dV)_B$ is the yield strain energy density, the rock elements are in the elastic state without damage;

(2) When $(dW/dV) \geq (dW/dV)_B$, the rock elements begin to damage and the internal cracks begin to form, the damage destruction status is represented by damage variable D ;

(3) When $(dW/dV) \geq (dW/dV)_D = \int_0^{\varepsilon_o} \sigma_{ij} d\varepsilon_{ij}$ (ε_o is the residual strain in the stress process), $(dW/dV)_D$ is the residual strain energy density, the macro crack coalescence is emerged and the rock mass enters into the plastic bearing region;

(4) When $(dW/dV) \geq (dW/dV)_E = \int_0^{\varepsilon_u} \sigma_{ij} d\varepsilon_{ij}$ (ε_u is the ultimate strain in the stress process), $(dW/dV)_E$ is the ultimate strain energy density, the rock mass is in the plastic flow stage. In the numerical calculation, in order to maintain the integrity of the entire calculation and the continuity of the rock element, a small residual modulus is given to the completely fractured rock element according to the results of the laboratory test, which is $E_c^* = 0.05E$.

4. Numerical analysis of zonal disintegration

4.1. Numerical Simulation process of zonal disintegration

In the ABAQUS calculation process, the generalized equivalent stress and strain containing the strain gradient of the elastoplastic stress state are calculated. If the stress state meets the tensile strength, the

rock element enters the tensile damage state, if the stress is less than the ultimate tensile strength, the strain energy density failure criterion is used to calculate the failure mode of the rock mass. The calculation process of the above idea in ABAQUS is shown in Fig. 3.

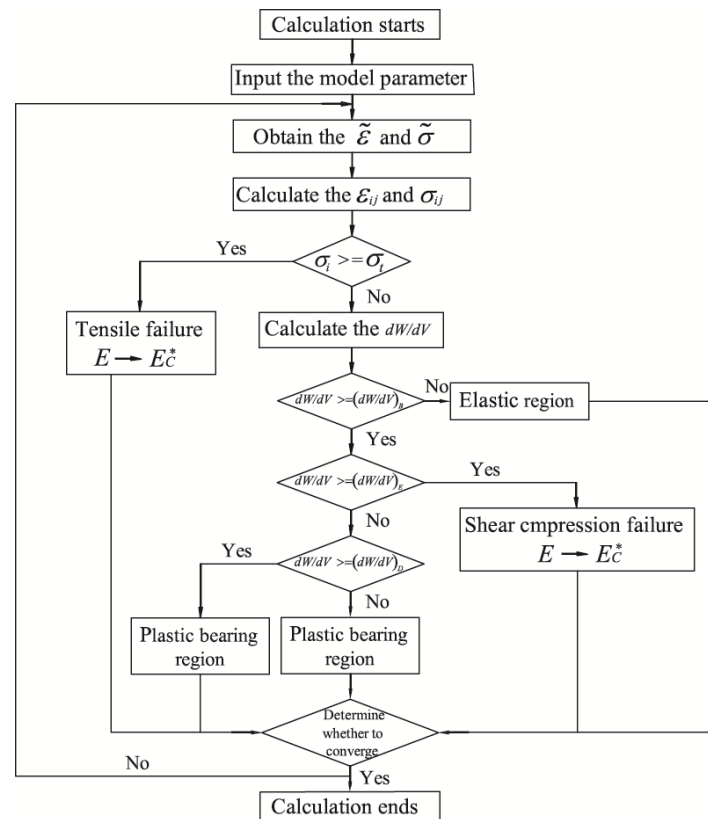


Figure 3. Flow chart of numerical implementation in ABAQUS

4.2. Comparison between model test results and numerical simulation results

Taking the geomechanical model test [22] as an example, numerical simulation size is 30m×30m×30m, the cavern section is circular and the radius of cavern is 2.5m, 17340 elements are divided, the specific calculation model is shown in Fig.4.

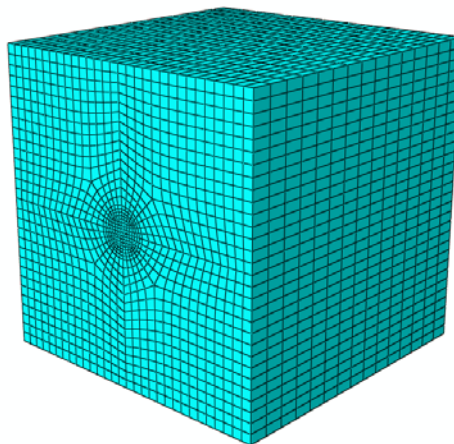


Figure 4. Three dimensional computational mesh of rock mass in ABAQUS

According to the model test, the initial elastic modulus is $E=77.82\text{GPa}$, the poisson's ratio is $\nu=0.268$, the density rock is $\rho=2620\text{kg/m}^3$, the compressive strength is $\sigma_c=88.55\text{MPa}$, the tensile strength is $\sigma_t=14.01\text{MPa}$. The depth of carven is -910m , the lithology is sandy mudstone and the initial stress is 23.36MPa , the side pressure coefficient is $k=1.5$, the stress parallel to the carven axis is 2 times the compressive strength.

After calculation, the calculation results shown in Fig. 5 can be obtained.

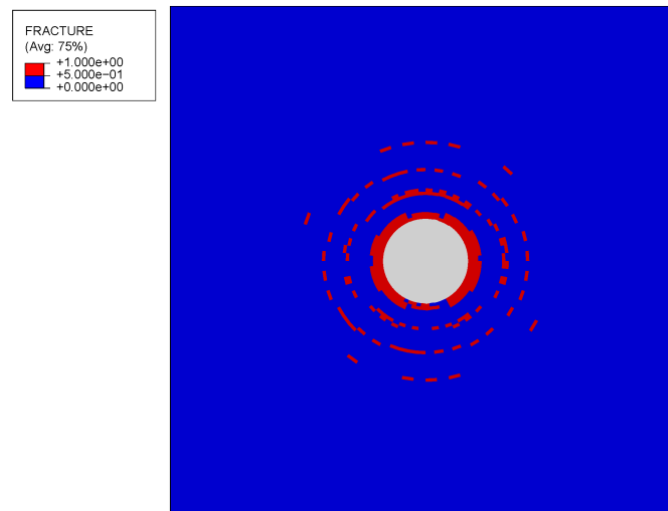


Figure 5. Failure states near the cavern

As can be seen from Fig.5, there are four fractured zones at the periphery of the cavern. The first fractured zone is the most severely damaged, and the fourth fractured zone has a smaller and dispersive range of damage zones, and it is more practical with the model test results. The first fractured zone ranged from 2.50m to 3.60m , the second fractured zone ranged from 4.20m to 4.50m , the third fractured zone ranged from 6.40m to 6.60m , and the fourth fractured zone ranged from 8.50m to 8.93m .

Tab.1 shows the comparison between numerical calculation and model test results [22]. Through the comparison of the data in the table, it is found that the average range and width of the fractured zone obtained by numerical calculation are basically consistent with the model test results, indicating that the calculation method is correct and feasible.

Table 1. Ranges of zonal disintegration obtained by numerical calculation and model test result

Number of fractured zones	Average radius/m		Average width/m	
	Model test results	Numerical calculation	Model test results	Numerical calculation
1	3.15	3.05	1.30	1.10
2	4.48	4.35	0.25	0.30
3	6.13	6.50	0.15	0.20
4	8.35	8.57	0.10	0.15

5. Conclusion

(1) Comparison between numerical simulation results and model test results, it can be seen that they are in good agreement. The elastoplastic damage softening model and calculation method are proved correctly and feasibly to simulate the zonal disintegration of deep rock mass.

(2) The numerical methods and failure criteria of rock mass are established to determine the evolution of the zonal disintegration during the excavation of the deep rock mass, and the width and number of fractured zones can be obtained.

(3) Since this numerical method is based on the FORTRAN language in ABAQUS, the numerical calculation has a wider application than the analytical method, which can be directly used to solve various complex engineering problems.

Acknowledgments

This work was financially supported by the National Key Research and Development Program of China (No. 2016YFC0401804-03), the Project of Taishan scholar Engineering, the National Natural Science Foundation of China (No. 41772282), the Preliminary Research Project of the Underground Experimental Project for the Geological Disposal of High-level Radioactive Waste (No. YKKY-J-2015-25). The authors are deeply grateful for the support.

References

- [1] Qian Qi-hu. The current development of nonlinear rock mechanics: The mechanics problems of deep rock mass [C]// Proceedings of the 8th Rock Mechanics and Engineering Conference. Beijing: Science Press, 2004: 10-17.
- [2] SHEMYAKIN E I, FISENKO G L, KURLENYA M V, et al. Zonal disintegration of rocks around underground workings, part I: data of in-situ observations [J]. Soviet Mining, 1986, 22 (3): 157-168.
- [3] LI Shu-cai, WANG Han-peng, QIAN Qi-hu, et al. In-situ monitoring research on zonal disintegration of surrounding rock mass in deep mine roadways[J]. Chinese Journal of Rock Mechanics and Engineering, 2008, 27 (8): 1545-1553.
- [4] GU Jin-cai, GU Lei-yu, CHEN An-min, et al. Model test study on mechanism of layered fracture within surrounding rock of tunnels in deep stratum [J]. Chinese Journal of Rock Mechanics and Engineering, 2008, 27 (3): 433-438.
- [5] ZHANG Qiang-yong, CHEN Xu-guang, LIN Bo, et al. Study of 3D geomechanical model test of zonal disintegration of surrounding rock of deep tunnel [J]. Chinese Journal of Rock Mechanics and Engineering, 2009, 28 (9): 1757-1 766.
- [6] GAO Fu-qiang, KANG Hong-pu, LIN Jian, Numerical simulation of zonal disintegration of surrounding rock mass in deep mine roadways [J]. Journal of China Coal Society, 2010, 35 (1): 21-25.
- [7] P. Jia, T. H. Yang, Q. L. Yu. Mechanism of parallel fractures around deep underground excavations [J]. Theoretical and Applied Fracture Mechanics, 2012, (61): 57-65.
- [8] CHEN Sheng-hong, WANG Hong-ru, XIONG Wen-lin. The effect of couple stress on jointed rock mass [J]. Journal of Hydraulic Engineering, 1990, (1): 44-48.
- [9] ZHANG Xutao, ZHANG Qiang-yong, XIANG Wen, et al. Zonal disintegration mechanism based on strain gradient theory [J]. Rock and Soil Mechanics, 2014, 35(4): 724-734.
- [10] HE Man-chao, XIE He-ping, PENG Su-ping, et al. Study on rock mechanics in deep mining engineering [J]. Chinese Journal of Rock Mechanics and Engineering, 2005, 24 (16): 2803-2813.
- [11] Zhang JW. Theoretical analysis on failure zone of surrounding rock in deep large-scale soft rock roadway [J]. Journal of China University of Mining and Technology, 2017, 46 (2): 292-299.
- [12] Pan Y, Wang ZQ, Wang ZQ. Study on stress Distribution of surrounding rock and work condition of tunnel based on strain nonlinear hardening and softening [J]. Chinese Journal of Rock Mechanics and Engineering, 2006, 25 (7): 1343-1351.
- [13] Cao RL, He SH, Wei J. Study of modified statistical damage softening constitutive model for rock considering residual strength [J]. Rock and Soil Mechanics, 2013, 34 (6): 1652-1660, 1667
- [14] M.G.D. Geers. Experimental Analysis and Computational Modelling of Damage and Fracture

- [D]. Eindhoven University of technology, 1997
- [15] KOHN R, TEMAM R. Dual spaces of stresses and strains, with applications to hencky plasticity [J]. APPLIED MATHEMATICS AND OPTIMIZATION, 1983, 10(1): 1-35.
- [16] Pan Y, Wang ZQ. Elastoplastic analysis of surrounding rock of circular chamber based on strain nonlinear softening [J]. Chinese Journal of Rock Mechanics and Engineering, 2005, 24 (6): 915-920.
- [17] Mindlin R D. Micro-structure in linear elasticity. Archive for Rational Mechanics and Analysis, 1964, 16 (1), 51-78.
- [18] Mindlin R D. Second gradient of strain and surface tension in linear elasticity. International Journal of Solids and Structures, 1965, 1(4), 417-438.
- [19] Jidong Zhao, Dorival Pedroso. Strain gradient theory in orthogonal curvilinear coordinates[J]. International Journal of Solids and Structures, 2008. 45 (11-12): 3507-3520.
- [20] Fleck N. A, Hutchinson J. W. A phenomen-ological theory for strain gradient effects in plasticity[J]. J Mech Phys Solids, 1993, 41 (12): 1825-1857.
- [21] G.C.Sih. Some basic problems in fracture mechanics and new concepts [J]. Engineering Fracture Mechanics, 1973, 5(2), 365-377.
- [22] Zhang Q Y, Zhang X T, Xiang W, et al. Model test study of zonal disintegration in deep rock mass under different cavern shapes and loading conditions [J]. Chinese Journal of Rock Mechanics and Engineering, 2013, 32 (8): 1564-1571.